Heart, Lung and Circulation (2019) **28,** 1587–1597
1443-9506/04/$36.00
https://doi.org/10.1016/j.hlc.2018.08.002

ORIGINAL ARTICLE

Dissecting Molecular Mechanisms Underlying Pulmonary Vascular Smooth Muscle Cell Dedifferentiation in Pulmonary Hypertension: Role of Mutated Caveolin-1 (Cav1^{F92A})-Bone Marrow Mesenchymal Stem Cells

Wancheng Yu, MD [a], Haiying Chen, PhD [b], Hongli Yang, MSc [b], Jie Ding, MSc [b], Peng Xia, MD [c], Xu Mei, PhD [d], Lei Wang, MD [c], Shuangfeng Chen, MD [b], Chengwei Zou, MD [a], Le-Xin Wang, PhD, FCSANZ [c,e*]**

[a]Department of Cardiac Surgery, Provincial Hospital Affiliated to Shandong University, Shandong 250021, China
[b]Central laboratory of Liaocheng People's Hospital, Liaocheng, Shandong, 252000, China
[c]Department of Cardiology, Liaocheng People's Hospital and Affiliated Liaocheng People's Hospital of Shandong University, Liaocheng, Shandong, 252000, China
[d]Department of Geriatrics, Shandong University Qilu Hospital, Shandong, China
[e]School of Biomedical Sciences, Charles Sturt University, Wagga Wagga, NSW, Australia

Received 11 February 2018; received in revised form 29 July 2018; accepted 14 August 2018; online published-ahead-of-print 7 September 2018

Background Pulmonary arterial hypertension (PAH) is characterised by remodelling in vascular smooth muscles, and switching from contractile (differentiated) to synthetic (dedifferentiated) phenotype. This study aimed to investigate the effect of a mutated caveolin-1 (Cav1^{F92A}) gene from bone marrow mesenchymal stem cells (rBMSCs) on phenotypic switching in the smooth muscle cells during PAH.

Methods Human pulmonary smooth muscle cells (HPASMCs) were treated with monocrotaline (MCT,1 μM), and co-cultured with Cav1^{F92A} gene modified rBMSCs (rBMSCs/Cav1^{F92A}). The nitric oxide (NO) production, cell adhesion, cell viability and inflammatory cytokines expression in rBMSCs was measured to evaluate the survival rate of rBMSCs and the changes of inflammatory cytokines. The concentration of NO/cGMP (nitric oxide/Guanosine-3′,5′-cyclic monophosphate), the tumour necrosis factor-alpha (TNF-α), transforming growth factor-beta1 (TGF-β1) mRNA, the expression of contractile smooth muscle cells (SMCs) phenotype markers (thrombospondin-1 and Matrix Gla protein, MGP), the synthetic SMCs phenotype markers

Abbreviations: PAH, Pulmonary arterial hypertension; Cav1^{F92A}, Mutated caveolin-1; HPASMCs, Human Pulmonary Artery Smooth Muscle Cells; MCT, Monocrotaline; rBMSCs, Rat bone marrow mesenchymal stem cells; SMCs, Smooth muscle cells; MGP, Matrix Gla protein; IL-4, Cytokines interleukin-4; INF-γ, Interferon-γ; NO, Nitric oxide; eNOS, Endothelial nitric oxide synthase; VSMC, Vascular smooth muscle cells; DMEM/F-12, Dulbecco's Modified Eagle Media/Nutrient Mixture F12

*Corresponding author at: Liaocheng People's Hospital, China. Tel.: +61 269 332905; Fax: +61 269 332587., Email: lwang@csu.edu.au
**Corresponding author at: Provincial Hospital Affiliated to Shandong University, China. Tel.: +61 269 332905; Fax: +61 269 332587., Email: zouchengwei@sdu.edu.cn

(H-caldesmon and smooth muscle gene SM22 alpha, SM22α), cell migration and the morphological changes in rBMSCs/Cav1^{F92A} co-cultured HPASMCs were investigated.

Results Cav1^{F92A} increased NO concentration, cell adhesion, cell viability, anti-inflammatory cytokines interleukin-4 (IL-4), and interleukin-10 (IL-10), but decreased the inflammatory cytokines interleukin-1α (IL-1α), interferon-γ (INF-γ) and TNF-α expression in rBMSCs. rBMSCs/Cav1^{F92A} activated the NO/cGMP, down-regulated TNF-α, TGF-β1, thrombospondin-1 and MGP expression, up-regulated SM22α and H-caldesmon expression, restored cell morphology, and inhibited cell migration in MCT treated HPASMCs.

Conclusions rBMSCs/Cav1^{F92A} inhibits switching from contractile to synthetic phenotype in HPASMCs. It also inhibits migration and promotes morphological restoration of these cells. rBMSCs/Cav1^{F92A} may be used as a therapeutic modality for PAH.

Keywords Nitric oxide • Human pulmonary artery smooth muscle cells • Rat bone marrow mesenchymal stem cells • Mutation caveolin-1(Cav1^{F92A}) • Phenotypic switching

Introduction

Pulmonary arterial hypertension (PAH) is characterised by smooth muscle remodelling of the pulmonary arteries [1]. The homeostatic imbalances, such as phenotypic dedifferentiation in pulmonary smooth muscle cells, are considered a primary cause for PAH [2]. Pulmonary smooth muscle cells maintain the ability of proliferation during switching from contractile to synthetic phenotype [3], which plays a critical role for the development of PAH [4]. Phenotypic switching in pulmonary smooth muscle cells leads to structural remodelling, enhanced cell proliferation and migration [5]. These changes result in concentric medial thickening of small arterioles, neovascularisation of nonmuscular capillary-like vessels, and structural changes in larger pulmonary arteries [4]. Therefore, regulating phenotypic switching of pulmonary smooth muscle cells may be a useful strategy in the prevention or treatment of PAH.

Current evidence suggests that inflammation plays a significant role in various types of PAH [6,7]. Inflammatory infiltrates in the lungs could stimulate the structural remodelling in the vasculature [8], and contribute to the pathogenesis of PAH by mediating phenotypic switching in pulmonary smooth muscle cells [9]. Nitric oxide (NO) has been shown to reduce lung inflammation [8], and regulate vascular smooth muscle cells proliferation, migration and differentiation [10,11]. Caveolin-1 (Cav1) plays an important role in suppressing endothelial nitric oxide synthase (eNOS) activity, and leading to decreased NO production [12]. Our recent study showed that substitution of alanine for phenylalanine produces a noninhibitory and mutated caveolin-1 (Cav1^{F92A}), which modifies rat bone marrow mesenchymal stem cells (rBMSCs), increasing endothelial nitric oxide synthase (eNOS) expression and NO production [13]. The mutated caveolin-1 (Cav1^{F92A}) also inhibits proliferation of smooth muscle cells in the pulmonary vasculature, and improves pulmonary haemodynamics [13].

Therapies with mesenchymal stem cells (MSCs) is an attractive option for the management of cardiovascular disease such as PAH [14,15]. The effect of Cav1^{F92A} gene modified rBMSCs (rBMSCs/Cav1^{F92A}) on phenotypic switching in Human Pulmonary Artery Smooth Muscle Cells (HPASMCs) has not yet been studied. Monocrotaline (MCT) is a poisonous crystalline alkaloid extracted from a leguminous plant of the genus *Crotalaria* (*C. spectabilis*) or the same genus of other plants. It can result in dysfunction of pulmonary artery endothelial cells and smooth muscle cells, which leads to intimal hyperplasia of the pulmonary artery and vascular remodelling[16]. MCT induced PAH is similar to human PAH [17]. In the present study, we investigated the effect of rBMSCs/Cav1^{F92A} on phenotypic switching in HPASMCs treated with MCT *in vitro*, to provide evidence for *in vivo* studies on PAH in the future.

Materials and Methods

Cell Culture

Human pulmonary artery smooth muscle cells were obtained from Sciencell (Sciencell Research Laboratories, Inc., San Diego, CA, USA), and cultured with Smooth Muscle Cell Growth Supplement. (Sciencell Research Laboratories, Inc., Beijing Solarbio Science & Technology Co., Beijing, China). Rat bone marrow mesenchymal stem cells were isolated, cultured as we described previously [13]. Briefly, rBMSCs were cultured in Dulbecco's Modified Eagle Media/Nutrient Mixture F12 (DMEM/F-12) (M&C Gene Technology [Beijing] LTD., Beijing, China), supplemented with 10% fetal bovine serum (FBS, Hyclon) and 1% penicillin/streptomycin (Beijing Solarbio Science & Technology Co., LTD., Beijing, China). Cells were maintained in 37 °C at a humidified atmosphere of 5% CO_2. The wild type Cav1-GFP plasmid was purchased from Addgene (Cambridge, MA, USA). The lentiviral packaging plasmids psPax2, pRSV-Rev, VSV-G were given as a kind gift by Dr Padraig Strappe (Central Queensland University, Rockhampton, Qld, Australia). The pLVX-mCMV-mCherry lentiviral vector backbone, pLVX- Cav1-mCMV-ZsGreen (LV-Cav1) and pLVX-Cav1^{F92A}-mCMV-mCherry (LV-Cav1^{F92A}) lentiviral vector was purchased from Biowit Technologies (Shenzhen, China).

Identification of rBMSCs

The cultured rBMSCs (1×10^6/ml) were trypsinized, washed with PBS and stained for 30 minutes at 37 °C in the dark with the following antibodies: anti-CD29-BV421™, anti-CD 34-PE, anti-CD44-FITC, anti-CD 45-PE, anti-CD 73-V450™ and anti-CD 90-BV480™ (all from BD Biosciences PharMingen, San Diego, CA, USA). Cell surface markers were analysed by flow cytometry (Becton, Dickinson, NJ, USA) and data analyses were conducted using BD FACSDiva (BD Biosciences, San Jose, CA, USA) software.

For osteogenic differentiation, rBMSCs (2×10^5/ml) were cultured with complete Dulbecco's Modified Eagle Media (DMEM) medium (Shanghai Biotech Co., Shanghai, China), containing 10% FBS and 1% penicillin/streptomycin supplemented with dexamethasone (100 nM), beta-Glycerol phosphate (10 mM) and ascorbic acid 2-phopshate (200 μM, all from Sigma–Aldrich, St. Louis, MO, USA). The media were changed every 3 days. Calcium deposits were detected in the extracellular matrix with 2% Alizarin Red S (Sigma–Aldrich) after 21 days of osteogenic differentiation, and stained for bright orange-red. For adipocyte differentiate, cells (2×10^5/ml) were incubated with adipogenic induction media (containing complete DMEM medium supplemented with dexamethasone (1 μM), 3-isobutyl-1-methylxanthine (IBMX, 0.5 mM), insulin [10 μg/ml], rosiglitazone [0.5 μM], and indomethacin [100 μM, all from Sigma–Aldrich]) for 3 days, and incubated with maintenance medium (containing complete DMEM medium) supplemented with insulin (10 μg/ml) for 14 days until fat droplets appeared. rBMSCs differentiation to adipocytes were confirmed by Oil Red O (Sigma–Aldrich) staining. Both Alizarin Red S and Oil Red O staining were visualised by light microscopy.

Lentiviral Vector Packaging and Transduction

Lentiviral vector packaging and transduction was performed as we described previously [18]. Briefly, lentiviral plasmids expressing the genes of interest (7 ug), together with packaging plasmids (3 ug pRSV-Rev, 3 ug VSV-G, 7 ug psPax2) were co-transfected into 293T cells (60–80% confluent), respectively, by lipofectamine 2000 (Thermo Fisher Scientific, MA, USA), per the manufacturer's instructions for the generation of LV-Cav1, LV-Cav1^{F92A}, or negative control LV-mCherry lentivirus (transfected with pLVX-mCMV-mCherry). The lentiviral particles were harvested at 48 hours and 72 hours post-transfection, and virus particles were concentrated by the PEG-it virus precipitation solution, following the manufacturer's instructions (SBI, New York, NY, USA). For rBMSCs transduction, the rBMSCs that grew at an exponential phase were randomly divided into the five groups: Control group, rBMSCs/Vector group (transduced with LV-mCherry lentivirus), rBMSCs/Cav1 group (transduced with LV-Cav1 lentivirus), rBMSCs/Cav1^{F92A} group (transduced with LV-Cav1^{F92A} lentivirus) and rBMSCs/Cav1^{F92A} + L-NAME group (transduced with LV-Cav1^{F92A} lentivirus and treated with L-NAME (2 mM, Beyotime Biotechnology, Jiangsu, China). The transduction efficiency was observed under fluorescent microscopy (CKX71, Olympus) 5 days post transduction.

NO Production, Cell Viability and rBMSCs Adhesion Assay

The nitrite, a stable end production of NO in the rBMSCs supernatants, was measured using a Nitric Oxide Colorimetric Assay Kit (Biovision, Milpitas, CA, USA) by Griess reaction and detected at 540 nm by Multiskan MK3 microplate reader. Cell viability in rBMSCs was detected by CCK-8 (Cell Counting Kit, Beyotime). The optical density of the well was measured at 450 nm using microplate reader. All experiments were performed in triplicate at least three times.

For cell adhesion assay, the Matrigel (BD Biosciences PharMingen, San Diego, CA, USA) was diluted with cold serum-free DMEM/F-12 at the ratio of 1:3. The mixed solution was added to 96-well plates (50 μl/well), and washed by PBS, then incubated with PBS containing 1% BSA in 37 °C. Each group of cells (2×10^4 cells/ml) was plated on matrigel-coated wells, then centrifuged (400 g × ,2 min) and incubated at 37 °C in 5% CO_2. After incubation for 20 minutes, the plate was vibrated twice (30 s/per each). After being washed with PBS, cells were fixed with100 μl paraformaldehyde for 15 minutes, stained with crystal violet for 15 minutes, washed with distilled water, and then 2% SDS was added in each well. The optical density (OD) was measured at 590 nm using a Multiskan MK3 microplate reader (Thermo Fisher Scientific, MA, USA). The experiment was performed in triplicate and repeated three times.

Cytokines Concentration in rBMSCs

The effect of rBMSCs/Cav1^{F92A} on the inflammatory cytokines concentration was measured by flow cytometry analysis. The supernatants in each group were collected after 5 days of transduction, cytokines concentration was measured using Cytometric Bead Array (CBA) Flex Set (BD Biosciences PharMingen, San Diego, CA, USA). The concentration of interleukin-4 (IL-4), interleukin-10 (IL-10), interferon-γ (INF-γ), interleukin-1α (IL-1α) and tumour necrosis factor-α (TNF-α) in cell supernatants were measured using flow cytometry. The data was analysed with a calibration curve prepared from serial dilutions of standard solution. Each experiment was repeated three times.

Co-Culture

HPASMCs were cultured in the lower compartment of a Millipore transwell-plate (Costar 3412, Corning Incorporated, NY, USA) and treated with MCT (1 μM) for 24 hours. Each group of rBMSCs (post-transduced 5 days) was placed onto 0.4 μm pore size polycarbonate membranes of the upper compartment in the transwell plate. Human pulmonary smooth muscle cells were evenly divided into six groups according to co-cultured rBMSCs transduced with different lentivirus in the upper compartment: Control group (only HPASMCs), Model group (only MCT-HPASMCs), Vector group (MCT-HPASMCs in the lower compartment and co-cultured with rBMSCs/Vector), Cav1 group (MCT-HPASMCs in the lower compartment and

co-cultured with rBMSCs/Cav1), $Cav1^{F92A}$ group (MCT-HPASMCs in the lower compartment and co-cultured with rBMSCs/$Cav1^{F92A}$), $Cav1^{F92A}$ + L-NAME group (MCT-HPASMCs in the lower compartment and co-cultured with rBMSCs/$Cav1^{F92A}$ and treated with eNOS inhibitor L-NAME).

NO Detection

The NO production in each group of HPASMCs was detected at 540 nm using Multiskan MK3 microplate reader. The relative content of NO in the cells was detected by a Nitric Oxide Colorimetric Assay Kit (Biovision Inc., Milpitas, CA, USA) using a Griess reaction. The concentration of nitrite was calculated using a linear calibration curve prepared from serial dilutions of nitrite standard solution. The experiments were performed in triplicate at least three times.

Quantitative Real-Time PCR (qPCR)

Total RNA was obtained from each group of HPASMCs by Trizol reagent (Tiangen Biotech Co., LTD, Beijing, China), then 1 μg of RNA was converted to cDNA and amplification was performed using Prime Script™ RT Master Mix (Takara Biotechnology, Dalian, China). Quantitative real-time PCR assays were performed in an Applied Biosystems 7500 (ABI 7500, USA) using SYBR Premix Ex Taq™ (TAKARA Biotechnology, Dalian, China). The relative genes expression was normalised to the GAPDH housekeeping gene by the $2^{-\triangle\triangle CT}$ method. Each experiment was repeated three times. All the Primers were purchased from Sangon Biotech, Shanghai, China. The sequences for Guanosine-3′,5′-cyclic monophosphate (cGMP), 5′- TGG AGG AGA ATA CTG GCA AGG −3′ (Sense) and 5′- TGG CTC TCT CCA CTG CTT CA −3′ (antisense), TNF-α, 5′- ACC TCC TCT CTG CCA TCA AG −3′ (Sense) and 5′- CTG AGT CGG TCA CCC TTC TC −3′ (antisense), transforming growth factor-beta1 (TGF-β1), 5′- GCA AGT GGA CAT CAA CGG GTT C −3′ (Sense) and 5′- CGC ACG CAG CAG TTC TTC TC −3′ (antisense), Thrombospondin-1, 5′- TCC TCC TCA CCC TTG ACA AC −3′ (Sense) and 5′- TGG ACA GCT CAT CAC AGG AG −3′ (antisense), Matrix Gla protein (MGP), 5′- CCC AGG AAT CAC ATG AAA GC −3′ (Sense) and 5′- TTC TCG GAT CCT CTC TTG GA −3′ (antisense), smooth muscle gene SM22 alpha (SM22α), 5′- TCC AGG TCT GGC TGA AGA AT −3′ (Sense) and 5′- GCT CCA TCT GCT TGA AGA CC −3′ (antisense), H-caldesmon were 5′- CTC GGA TCT TCC TGT TCC TG −3′ (Sense) and 5′- TTC AAG CCA GCA GTT TCC TT −3′ (antisense). All the primers were synthesised by the Shenggong Biological engineering technology company (Shanghai, China). The quality of primers was analysed by melting curve analysis. The melting curve was done showing no primer dimer and no other specific product. Each experiment was evaluated with three PCR reactions and each experiment was repeated three times.

Western Blot

The protein extracts were prepared by homogenisation in an ice cold lysis buffer including PMSF (Beyotime Biotechnology), then centrifuged (5 min, 4 °C and 12,000 g) before transferring the supernatant to new tubes. The protein concentration was analysed by BCA Protein Assay Kit (Beyotime Biotechnology). Equal amounts of protein (15 μg) were then separated by 10% SDS-PAGE and were electro-transferred to polyvinylidene difluoride (PVDF) membranes (Millipore Corp, Billerica, MA, USA) after electrophoresis. The PVDF membranes were incubated with 5% skimmed milk in TBST at room temperature for 1 hour, then incubated overnight at 4 °C with polyclonal antibody TNF-α (1:200 dilution, Boster Biological Technology, Wuhan, China), monoclonal antibody TGF-β1 (1:1000 dilution, Abcam, Cambridge, UK) and β-actin antibody (1:1000 dilution, Abcam). The PVDF membranes were incubated with goat anti-rabbit or goat anti-mouse IgG/HRP secondary antibodies (Beyotime, Biotechnology), respectively, diluted at a ratio of 1:1000 for one hour before washing with TBST three times. Protein bands were visualised using ECL western blotting kit (Beyotime Biotechnology). The intensity of resulting bands was measured by a densitometer, and analysed with AlphaView analysis software (ProteinSimle, San Jose, CA, USA). The values for proteins expression were normalised using β-actin.

Morphological Changes of HPASMCs and HPASMCs Migration Assay

Morphological changes of HPASMCs was investigated and photographed under fluorescent microscopy (CKX71, Olympus) after HPASMCs co-cultured with different gene modified rBMSCs for 72 hours. For HPASMCs migration Assay, 200 μl tips were utilised to draw the centreline of each well at the bottom of plates after the HPASMCs were co-cultured with each group of rBMSCs for 24 hours. The images were taken at 0 hours and 24 hours after scratch. The distance of wound healing was measured by Image-Pro Plus 6.0 software (Media Cybernetics, Silver Spring, MD, USA). Wound healing was calculated by the formula: wound healing (%) = [1-(wound area at T24 h/wound area at T0 h)] × 100%. A total of five areas were selected randomly from each well and the cells in three wells of each group were quantified.

Statistical Analysis

The values were expressed as means ± SD. The statistical significance of difference was calculated by one-way ANOVA, followed by SNK-q test using the SPSS 16.0 statistical package (IBM SPSS Statistics for Windows, Chicago, Il, USA). P value < 0.05 was considered statistically significant.

Results

Expression of Cell Surface Markers and Differentiation Ability of rBMSCs

Rat bone marrow mesenchymal stem cells surface markers CD34 (3.7%) and CD45 (23.9%), representing

haematopoietic cell-specific markers, were lower than in the isotype control. The percentage of the mesenchymal stem cell-specific markers CD29, CD73 and CD90 positive cells were more than 90%, and CD44 positive cells were nearly 90% (Figure 1A). Alizarin Red staining is one method that determines the osteogenic differentiation capability of rBMSCs, and the Alizarin red calcium deposition, the formation of calcium salt nodules was detected at day 21 after culture in osteoblast induction medium (Figure 1B). For adipogenic differentiation, a significant increase in Oil Red O absorbance was observed after 14 days incubated with adipogenic medium (Figure 1C). The imagines demonstrated that rBMSCs can differentiate to osteoblasts and adipocytes.

Lentiviral Vector Transduction Efficiency

Five (5) days post-transduction, the green fluorescence protein (ZsGreen) expression was detected in Cav1 groups. The expression of red fluorescence protein (mCherry) was detected in Vector groups and Cav1^{F92A} groups. The transduction efficiency was greater than 80% in all groups (Figure 1D).

Cav1^{F92A} Increased NO Production and cGMP mRNA Expression

Nitric oxide production was increased both in rBMSCs and HPASMCs by introduction of Cav1^{F92A} or co-cultured with rBMSCs/Cav1^{F92A}. Nitric oxide production in rBMSCs transduced with Cav1^{F92A} lentivirus was higher than control and

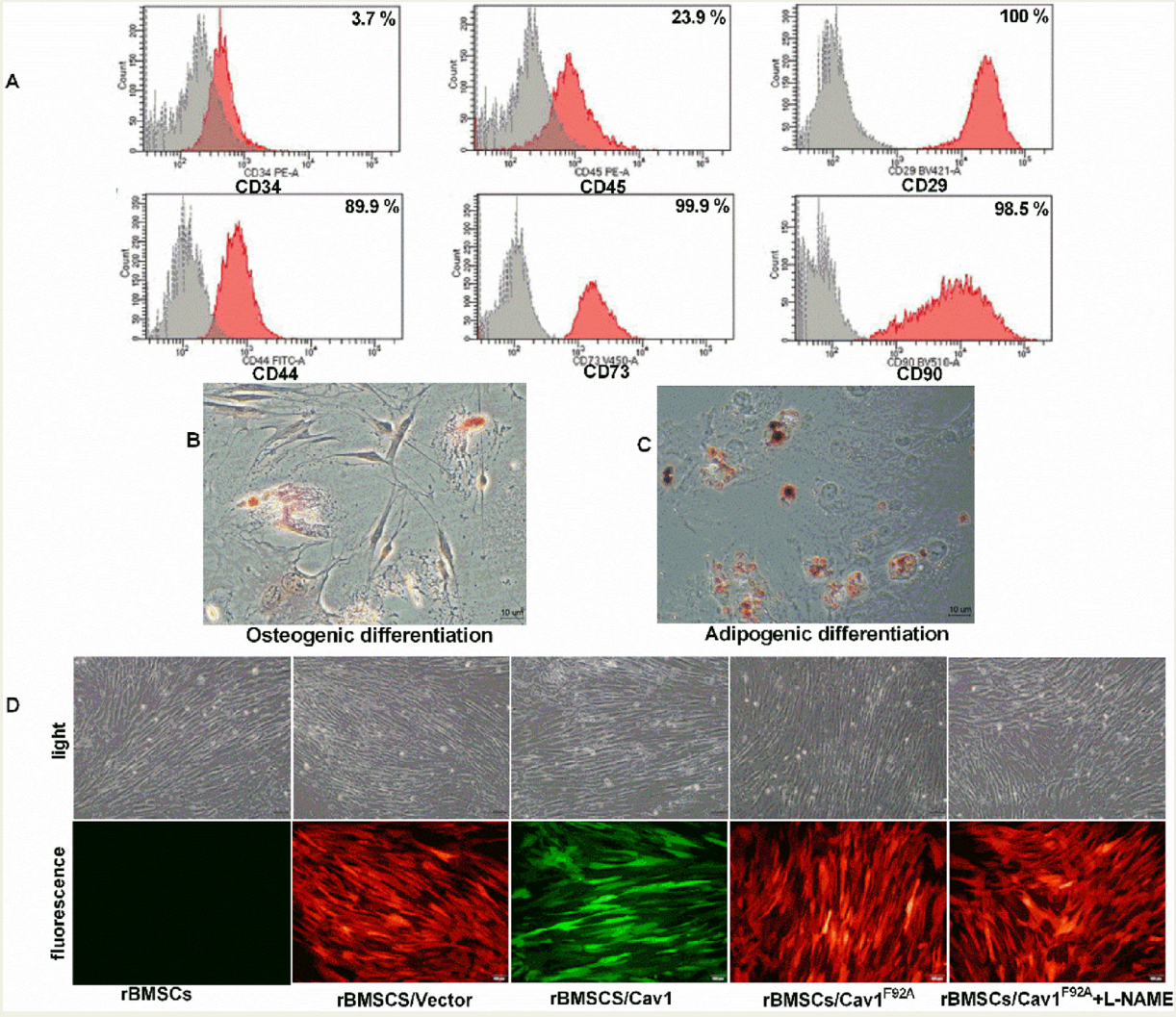

Figure 1 rBMSCs characterisation and transduction efficiency. A: The expression of cell surface markers in rBMSCs. It showed that the positive mesenchymal stem cell markers CD29 (+), CD90 (+), CD44 (+) and CD73 (+) were about 90%. The haematopoietic marker CD34 and CD45 positive cells were less than 4% and 24% respectively. B–C: Osteogenic and adipogenic differentiation of rBMSCS. rBMSCs were stained with Alizarin Red (B) and Oil Red O (C) respectively. Bar = 10 μm. D. Lentiviral vector transduction efficiency at 5 days post-infection (10 ×).
Abbreviations: rBMSCs, bone marrow mesenchymal stem cells.

Table 1 The effect of Cav1^{F92A} on NO production, cell adhesion and cell viability in rBMSCs (mean ± SD).

Groups	NO production (μM)	Cell adhesion (OD)	Cell viability (OD)
Control	4.836 ± 0.723	1.080 ± 0.075	1.069 ± 0.052
rBMSCs/Vector	5.153 ± 0.625[a]	1.231 ± 0.164[a]	1.188 ± 0.067[a]
rBMSCs/Cav-1	5.279 ± 0.674[a]	1.297 ± 0.205[a]	1.118 ± 0.072[a]
rBMSCs/Cav1^{F92A}	8.762 ± 0.127[cf]	2.105 ± 0.072[cf]	1.385 ± 0.056[ce]
rBMSCs/Cav1^{F92A} + L-NAME	3.872 ± 0.323[adi]	1.125 ± 0.079[adi]	1.167 ± 0.108[adh]

[a]$p>0.05$, [c]$p<0.01$ *vs.* control groups, [d]$p>0.05$, [e]$p<0.05$, [f]$p<0.01$ *vs.* rBMSCs/Cav-1, [h]$p<0.05$, [i]$p<0.01$ *vs.* rBMSCs/Cav1^{F92A}.
Abbreviations: rBMSCs, bone marrow mesenchymal stem cells; Cav1F92A, caveolin-1; OD, optical density; NO, nitric oxide.

rBMCSs/Cav1 groups ($p < 0.05$, Table 1). The same results were also found in HPASMCs, manifested above two-fold increase of NO level after HPASMCs co-cultured with rBMSCs/Cav1^{F92A}, compared to model groups ($p < 0.05$, Table 2). The NO production was decreased after HPASMCs co-cultured with rBMSCs/Cav1^{F92A} and treated with eNOS inhibitor L-NAME.

Nitric oxide has an impact on the pulmonary circulation mainly through the second messenger cGMP [8,19], and cGMP mRNA expression was elevated about 3.9-fold in HPASMCs co-cultured with rBMSCs/Cav1^{F92A} compared with model groups, but reduced after L-NAME treatment ($p < 0.05$, Table 2).

Cav1^{F92A} Enhanced Cell Adhesion and Viability in rBMSCs

Cell adhesion and viability was increased about two-fold and 1.3-fold, respectively, in rBMSCs/Cav1^{F92A} groups ($p < 0.05$, Table 1). They were both inhibited after L-NAME treatment ($p < 0.05$, Table 1).

Table 2 The effect of rBMSCs/Cav1^{F92A} on NO production and cGMP mRNA expression in MCT treated HPASMCs (mean ± SD).

Group	NO production (μM)	Folds change of cGMP
Control	3.389 ± 0.313	1.000 ± 0
Model	1.616 ± 0.088[c]	0.607 ± 0.016[c]
Vector	3.708 ± 0.196[cf]	1.072 ± 0.146[af]
Cav1	3.470 ± 0.204[af]	1.172 ± 0.069[af]
Cav1^{F92A}	7.460 ± 0.385[cfi]	2.374 ± 0.206[cfi]
Cav1^{F92A} + L-NAME	3.195 ± 0.104[afgl]	1.210 ± 0.054[afgl]

[a]$p>0.05$, [c]$p<0.01$ *vs.* control groups, [f]$p<0.01$ *vs.* model groups, [g]$p>0.05$, [i]$p<0.01$ *vs.* Cav-1 groups, [l]$p<0.01$ *vs.* Cav1^{F92A} groups.
Abbreviations: Cav1^{F92A}, caveolin-1; rBMSCs, bone marrow mesenchymal stem cells; MCT, monocrotaline; HPASMCs, human pulmonary smooth muscle cells; NO, nitric oxide; cGMP, Guanosine-3′,5′-cyclic monophosphate.

The Effect of rBMSCs/Cav1^{F92A} on the Expression of Inflammatory Cytokines

The IFN-γ, IL-1α and TNF-α were decreased while anti-inflammatory cytokine IL-4 and IL-10 were increased in rBMSCs/Cav1^{F92A} groups compared with the other four groups (Figure 2). Moreover, the levels of pro-inflammatory cytokines TNF-α, TGF-β1 mRNA and protein expression were increased in HPASMCs model groups (MCT-HPASMCs) (Figure 3), but were suppressed in HPASMCs co-cultured with rBMSCs/Cav1^{F92A} (Figure 3). The anti-inflammatory effect of Cav1^{F92A} was blocked by the eNOS inhibitor L-NAME in rBMSCs and HPASMCs groups (Figures 2, 3).

rBMSCs/Cav1^{F92A} Inhibited the HPASMCs Morphological Changes, Phenotypic Switching and Migration

In MCT-HPASMCs groups, the cells are fibroblasts-like and larger in volume, while the cells in control groups are spindle-shaped with smaller size. However, the cells were more spindle-shaped and smaller in HPASMCs co-cultured with rBMSCs/Cav1^{F92A} than in the model groups (Figure 4A). The expression of synthetic smooth muscle-specific marker thrombospondin-1 and MGP was up-regulated, but the SM22α and H-caldesmon were down-regulated in model groups compared with control groups (Figure 4B). Interestingly, MCT induced phenotypic switching from contractile to synthetic phenotype in HPASMCs was inhibited by co-culture with rBMSCs/Cav1^{F92A}, however, the L-NAME inhibited the function of rBMSCs/Cav1^{F92A} (Figure 4). Furthermore, for wound healing assay, the migration distance covered in model groups was narrower (migrated about 41.4% of the scratch) than that of the cells in the control groups at 24 hours. The cell migration was inhibited in rBMSCs/Cav1^{F92A} groups after HPASMCs co-cultured with rBMSCs/Cav1^{F92A} (Figure 5).

Discussion

The pathological phenotype of vascular wall in PAH seems to be triggered by different environmental stresses and

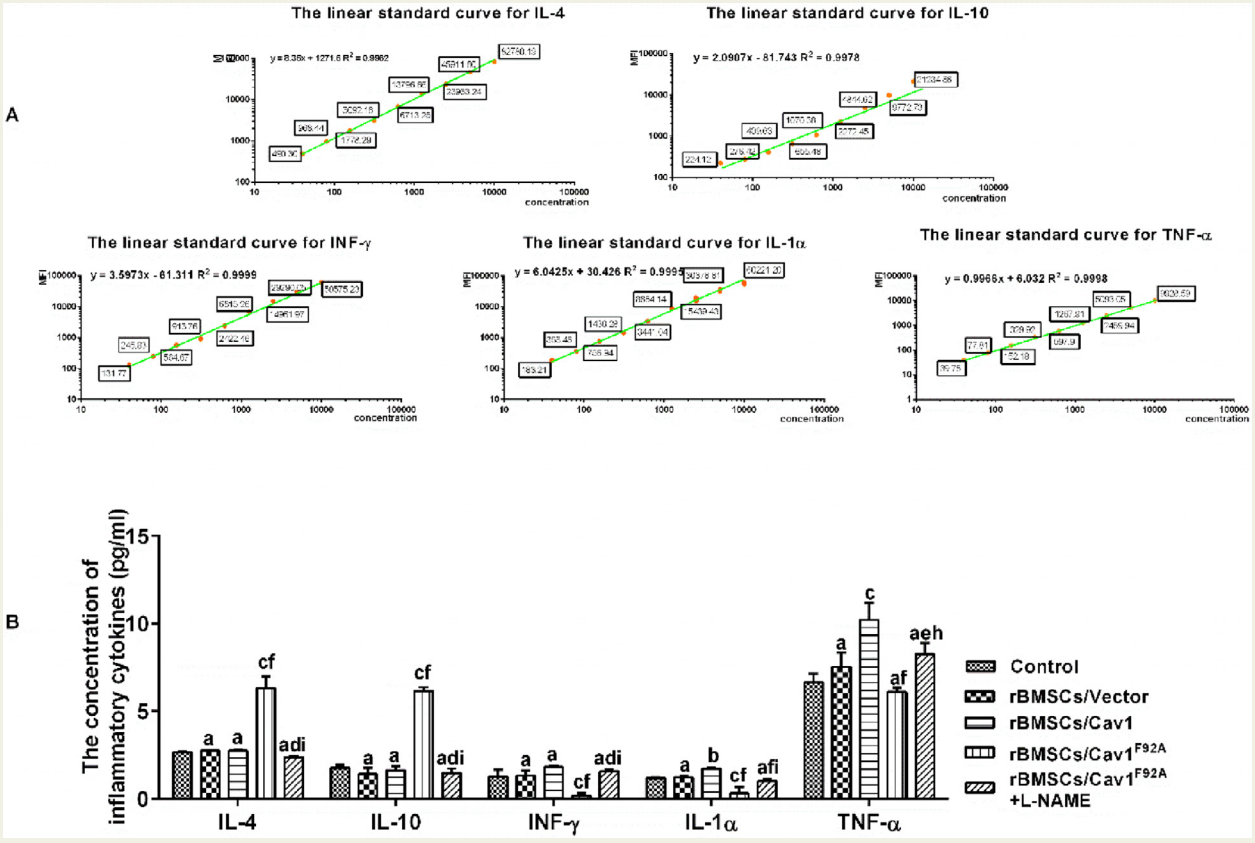

Figure 2 **The effect of Cav1^{F92A} on the inflammatory cytokines expression in rBMSCs**. A. The linear standard curves were established per the manuscript instruction. B. The concentration of inflammatory cytokines was calculated by the standard curves. $^{a}p > 0.05$, $^{b}p < 0.05$, $^{c}p < 0.01$ *vs.* Control groups, $^{d}p > 0.05$, $^{e}p < 0.05$, $^{f}p<0.01$ *vs.* rBMSCs/Cav-1, $^{h}p < 0.05$, $^{i}p < 0.01$ *vs.* rBMSCs/Cav1^{F92A}.
Abbreviations: Cav1^{F92A}, caveolin-1; rBMSCs, bone marrow mesenchymal stem cells.

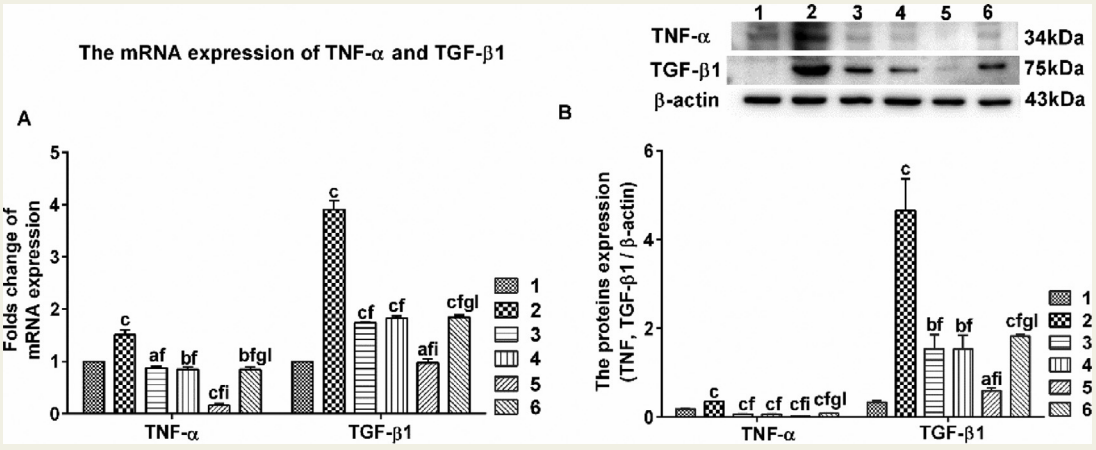

Figure 3 **rBMSCs/Cav1^{F92A} reduced the TNF-α and TGF-β1 expression in MCT treated HPASMCs**. A. The changes of TNF-α and TGF-β1 mRNA expression. B. The protein expression of TNF-α and TGF-β1. 1. Control group, 2. Model group, 3. Vector group, 4. Cav1 group, 5. Cav1^{F92A} group, 6. Cav1^{F92A} + L-NAME group. $^{a}p > 0.05$, $^{b}p < 0.05$, $^{c}p < 0.01$ *vs.* Control groups, $^{f}p < 0.01$ *vs.* Model groups, $^{g}p > 0.05$, $^{i}p < 0.01$ *vs.* Cav-1 groups, $^{l}p < 0.01$ *vs.* Cav1^{F92A} groups.
Abbreviations: Cav1^{F92A}, caveolin-1; rBMSCs, bone marrow mesenchymal stem cells.

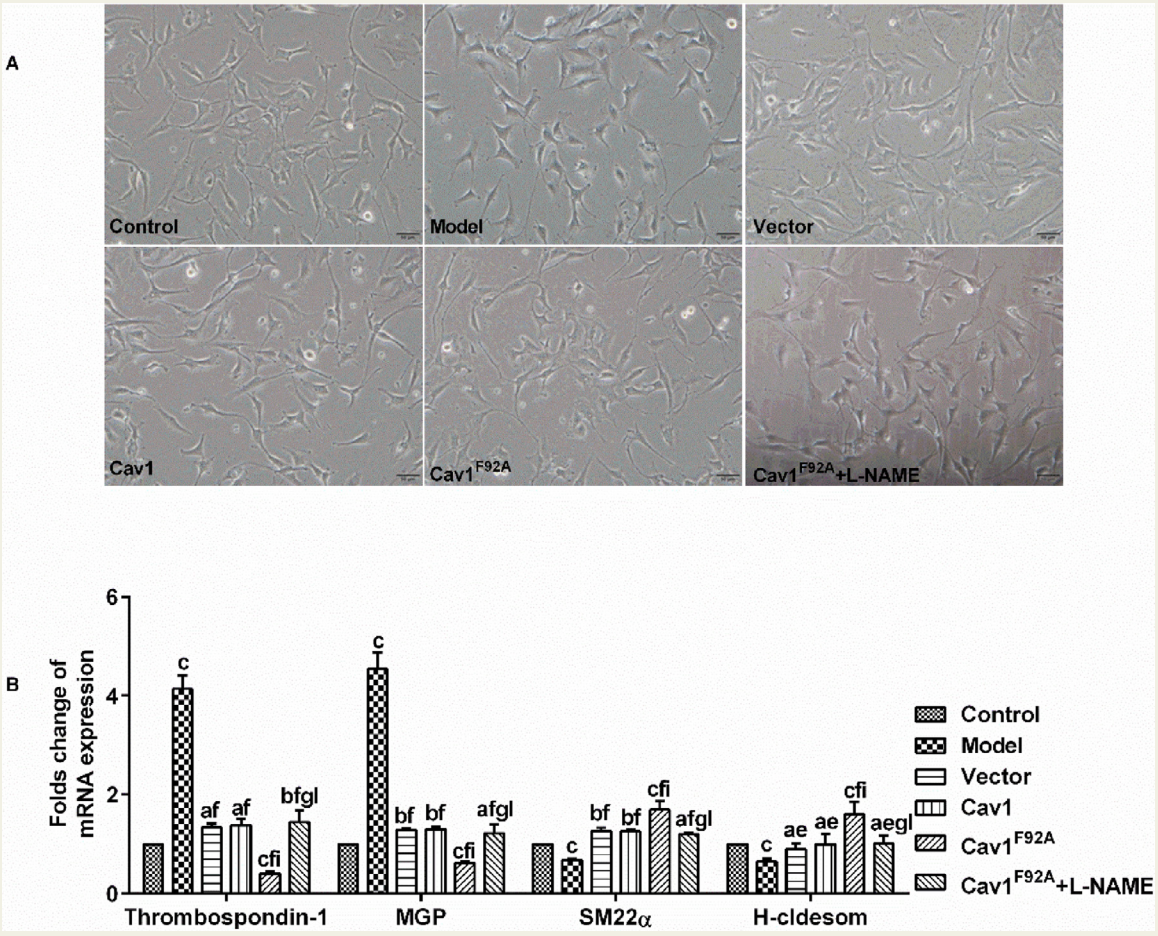

Figure 4 The effect of rBMSCs/Cav1^{F92A} on cell morphological changes and the phenotype marker genes expression in MCT treated HPASMCs. A. Cell morphological changes in MCT treated HPASMCs (20×). B: The change of SMCs phenotype markers expression. The contractile SMCs phenotype markers thrombospondin-1 and MGP was down-regulated, but the synthetic SMCs phenotype markers SM22α and H-caldesmon was up-regulated by rBMSCs/Cav1^{F92A}. $^{a}p > 0.05$, $^{b}p < 0.05$, $^{c}p < 0.01$ *vs.* Control groups, $^{e}p < 0.05$, $^{f}p < 0.01$ *vs.* Model groups, $^{g}p > 0.05$, $^{i}p < 0.01$ *vs.* Cav-1 groups, $^{l}p < 0.01$ *vs.* Cav1^{F92A} groups.

Abbreviations: SMCs, smooth muscle cells; Cav1^{F92A}, caveolin-1; rBMSCs, bone marrow mesenchymal stem cells; MCT, monocrotaline; HPASMCs, human pulmonary smooth muscle cells; MGP, matrix Gla protein.

injuries, including increased inflammation [20]. Endothelial cells injury and apoptosis is one of the first events to occur [20], leading to endothelial dysfunction, phenotypic change of cells and decreased NO release [20,21]. A previous study has found that mutation of Cav1 scaffold domain phenylalanine at position 92 (F92) to alanine has been shown to reduce inhibitory actions of Cav1 toward eNOS, and enhance NO generation [12]. Nitric oxide exhibits diverse physiological actions, including vasodilation, anti-inflammation, anti-platelet, inhibiting proliferation and migration [22]. Phenotypic changes of SMCs from contractile to synthetic phenotype is one of the characteristics of PAH. In the present study, we found that rBMSCs/Cav1^{F92A} inhibited the phenotypic switching from contractile to synthetic phenotype in MCT treated HPASMCs by enhanced NO production.

Mesenchymal stem cells treatment is a promising strategy for PAH due to its multidirectional differentiation and proliferative ability [14], but the low survival rate of transplanted cells limited its application [23]. Therefore, it is important to enhance MSCs adhesion to promote cell survival [24]. Our results showed that Cav1^{F92A} promoted the NO generation and the adhesion of rBMSCs, resulting in increased cell viability. This increased cell survival rate may have significant implications for stem cell therapy for PAH and other cardiovascular disorders.

Activation of inflammatory processes is associated with development of PAH [25]. The present study found that Cav1^{F92A} had an inhibitory effect on inflammatory cytokines, down-regulating expression of pro-inflammatory cytokines IL-1α, INF-γ, and TNF-α, but up-regulating the expression of anti-inflammatory cytokines IL-4 and IL-10 in rBMSCs/Cav1^{F92A} groups. Furthermore, pro-inflammatory cytokines TNF-α and TGF-β1 in HPASMCs co-cultured with rBMSCs/Cav1^{F92A} were also decreased. The pro-inflammatory

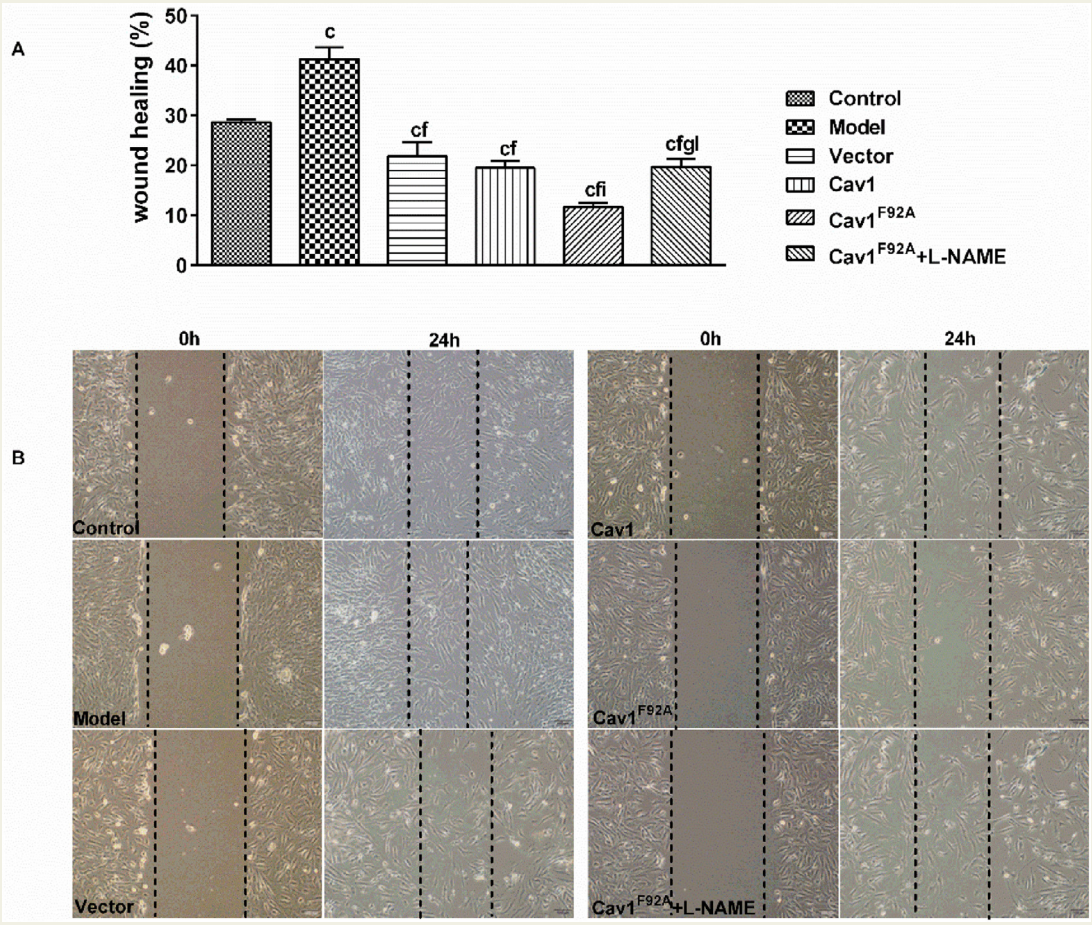

Figure 5 Cell migration in HPASMCs. Images were taken at 0 h and 24 h after scratching (10 ×). $^{c}p < 0.01$ *vs.* control groups, $^{f}p < 0.01$ *vs.* model groups, $^{g}p > 0.05$, $^{i}p < 0.01$ *vs.* Cav-1 groups, $^{l}p < 0.01$ *vs.* Cav1^{F92A} groups.
Abbreviations: Cav1^{F92A}, caveolin-1; HPASMCs, human pulmonary smooth muscle cells.

cytokines INF-γ, IL-1α, TNF-α and TGF-β1 were associated with pulmonary inflammation [26,27]. The macrophages, activated by IFN-γ and TNF-α, exert tumouricidal effects by producing IL-12p40 [26], which contributes to the inflammatory response [28]. In addition, the activated macrophages can synthesise inflammatory cytokines, such as IFN-γ, TNF-α, IL-6, which sustain the chronic inflammation [26]. TNF-α expression correlates with TGF-β1 mRNA expression and induction of TGF-β1 [29]. TGF-β1 stimulates pulmonary inflammation, fibrosis, myofibroblast accumulation and alveolar destruction [30]. Therefore, the increased TNF-α and TGF-β1 in MCT treated HPASMCs may lead to severe inflammation. The inflammation in pulmonary disease resulted from epithelial injury, mediating phenotypic switching in pulmonary vascular smooth muscle cells, contributing to lung remodelling [9,31]. IL-4, IL-10 were the anti-inflammatory cytokines, among which IL-10 is a pleiotropic anti-inflammatory cytokine with vascular protective properties [32]. Moreover, IL-10 can antagonise IFN-γ activated macrophages and TNF-α production by its suppressive effect on immunity [33]. Therefore, the elevated anti-inflammatory cytokines IL-4, IL-10 and reduced pro-inflammatory cytokine INF-γ, IL-1α and TNF-α in rBMSCs/Cav1^{F92A}, together with the increased concentration of NO and elevated cGMP in HPASMCs, may lead to less inflammation, less vascular tension and phenotypic switching.

Phenotypic switching of HPASMCs plays a crucial role in the pathogenesis of PAH [3]. In the present study, the morphological restoration, the up-regulated HPASMCs contractile genes (thrombospondin-1, MGP), the down-regulated synthetic (or differentiated) genes (SM22α, H-caldesmon), and the repressed HPASMCs migration manifested the inhibited phenotypic switching in MCT treated HPASMCs by rBMSCs/Cav1^{F92A}. Smooth muscle cells possess a remarkable phenotypic plasticity that allows rapid adaptation to fluctuating environmental cues [34]. Persistent pulmonary hypertension results in vascular wall fibrosis by inducing a phenotypic switching from contractile SMCs to synthetic SMCs, various phenotypic states are reflected by the expression of a distinct set of markers. It was reported that the SM22α, H-caldesom, smooth muscle alpha-actin (SM alpha-actin), smooth muscle myosin heavy chain (SM-MHC)

tropoelastin, a matrix protein, alpha-smooth muscle (SM) actin, calponin and phospholamban were all associated with the contractile function of contractile (differentiated) vascular SMCs, and the thrombospondin-1 and matrix Gla protein (MGP), osteopontin were associated with synthetic (dedifferentiated) function of the dedifferentiated vascular SMCs [35,36]. In our results, the reduced thrombospondin-1, MGP and elevated SM22α, H-caldesom in MCT-HPASMCs co-cultured with rBMSCs/Cav1^{F92A} manifested the regulation effect of rBMSCs/Cav1^{F92A} on phenotypic switching by increased NO production.

It has been suggested that NO has an impact on the progression of PAH by mediating phenotypic switching induced by inflammation [37]. Phenotypic switching leads to migration and proliferation in pulmonary vascular smooth muscle cells, both contributing to the pathogenesis of PAH [37]. Matrix Gla protein (MGP) was involved in regulating the calcification that commonly occurs in vascular lesions [35]. For thrombospondin-1, it was involved in a number of cellular processes which regulate cell behaviour, including migration, mitogenesis, attachment and differentiation [38]. The increased thrombospondin-1 could enhance the migration and proliferation of SMCs [39]. Consistent with above studies, MCT-HPASMCs co-cultured with rBMSCs/Cav1^{F92A} inhibited cell migration and reduced thrombospondin-1 expression, suggesting rBMSCs/Cav1^{F92A} may reduce the HPASMCs migration by regulating the contractile genes or synthetic genes. Moreover, the cell morphology changed significantly in MCT-HPASMCs groups; they were fibroblast-like and larger in volume, while the cells are spindle-shaped with smaller size in MCT-HPASMCs co-cultured with rBMSCs/Cav1^{F92A}, suggesting that the cells' morphological restoration was promoted by rBMSCs/Cav1^{F92A}. The SM22α and H-caldesom are the differentiated SMCs markers and characterised by its SMCs-specific expression pattern [40]. SM22-α is involved in maintaining and remodelling of smooth muscle cytoskeleton and contractility, and H-caldesmon is involved in regulation of SMCs contraction [40]. Such a phenotype is characterised by a spindle-shaped morphology, and contractile gene expression [40]. Thus, the decreased expression of SM22α and H-caldesom in MCT-HPASMCs groups exhibited an immature phenotype, but the phenotype was more mature in MCT-HPASMCs co-cultured with rBMSCs/Cav1^{F92A}, indicating that rBMSCs/Cav1^{F92A} had an inhibitory function on morphological changes.

Conclusions

The present study demonstrated that rBMSCs/Cav1^{F92A} inhibits switching from contractile to synthetic phenotype in human pulmonary arterial smooth muscle cells, by activating NO signalling pathways, stimulating anti-inflammatory cytokines, and suppressing the expression of pro-inflammatory cytokines. rBMSCs/Cav1F92A inhibiting also inhibits migration and promotes morphological restoration of the human pulmonary arterial smooth muscle cells. These results suggest that rBMSCs/Cav1^{F92A} plays a central role in the pathogenesis of MCT-induced pulmonary hypertension, and may be used as a therapeutic modality for pulmonary hypertension or other cardiovascular diseases.

Declarations

Funding

This work was supported by a grant from the National Natural Science Foundation of China (No. 81270104), the Natural Science Foundation of Shandong Province of China (No. ZR2016HP33, ZR2013HM056, ZR2017BH017), and the Shandong province science and technology development plan (2014GH218016)

References

[1] Nogueira-Ferreira R, Ferreira R, Henriques-Coelho T. Cellular interplay in pulmonary arterial hypertension: implications for new therapies. Biochim Biophys Acta 2014;1843(5):885–93.
[2] Shatat MA, Tian H, Zhang R, Tandon G, Hale A, Fritz JS, et al. Endothelial Kruppel-like factor 4 modulates pulmonary arterial hypertension. Am J Respir Cell Mol Biol 2014;50(3):647–53.
[3] Wang J, Yan CH, Li Y, Xu K, Tian XX, Peng CF, et al. MicroRNA-31 controls phenotypic modulation of human vascular smooth muscle cells by regulating its target gene cellular repressor of E1A-stimulated genes. Exp Cell Res 2013;319(8):1165–75.
[4] Aggarwal S, Gross CM, Sharma S, Fineman JR, Black SM. Reactive oxygen species in pulmonary vascular remodeling. Compr Physiol 2013;3(3):1011–34.
[5] Liu CP, Dai ZK, Huang CH, Yeh JL, Wu BN, Wu JR, et al. Endothelial nitric oxide synthase-enhancing G-protein coupled receptor antagonist inhibits pulmonary artery hypertension by endothelin-1-dependent and endothelin-1-independent pathways in a monocrotaline model. Kaohsiung J Med Sci 2014;30(6):267–78.
[6] Hassoun PM, Mouthon L, Barbera JA, Eddahibi S, Flores SC, Grimminger F, et al. Inflammation, growth factors, and pulmonary vascular remodeling. J Am Coll Cardiol 2009;54(1 Suppl):S10–9.
[7] Dorfmuller P, Perros F, Balabanian K, Humbert M. Inflammation in pulmonary arterial hypertension. Eur Respir J 2003;22(2):358–63.
[8] Crosswhite P, Sun Z. Nitric oxide, oxidative stress and inflammation in pulmonary arterial hypertension. J Hypertens 2010;28(2):201–12.
[9] Sun L, Zhao M, Liu A, Lv M, Zhang J, Li Y, et al. Shear stress induces phenotypic modulation of vascular smooth muscle cells via AMPK/mTOR/ULK1-mediated autophagy. Cell Mol Neurobiol 2018;38(2):541–8.
[10] Csiszar A, Labinskyy N, Olson S, Pinto JT, Gupte S, Wu JM, et al. Resveratrol prevents monocrotaline-induced pulmonary hypertension in rats. Hypertension 2009;54(3):668–75.
[11] Hamik A, Lin Z, Kumar A, Balcells M, Sinha S, Katz J, et al. Kruppel-like factor 4 regulates endothelial inflammation. J Biol Chem 2007;282(18):13769–7.
[12] Bernatchez P, Sharma A, Bauer PM, Marin E, Sessa WC. A noninhibitory mutant of the caveolin-1 scaffolding domain enhances eNOS-derived NO synthesis and vasodilation in mice. J Clin Invest 2011;121(9):3747–55.
[13] Chen H, Yang H, Yue H, Strappe PM, Xia P, Pan L, et al. Mesenchymal stem cells expressing eNOS and a Cav1 mutant inhibit vascular smooth muscle cell proliferation in a rat model of pulmonary hypertension. Heart Lung Circ 2017;26(5):509–18.
[14] Chen HY, Strappe PM, Wang LX. Stem cell therapies for cardiovascular diseases: what does the future hold? Heart Lung Circ 2017;26(3):205–8.
[15] Fischer UM, Harting MT, Jimenez F, Monzon-Posadas WO, Xue H, Savitz SI, et al. Pulmonary passage is a major obstacle for intravenous stem cell delivery: the pulmonary first-pass effect. Stem Cells & Development 2009;18(5):683–92.

[16] Thomas HC, Lamé MW, Dunston SK, Segall HJ, Wilson DW. Monocrotaline pyrrole induces apoptosis in pulmonary artery endothelial cells. Toxicol Appl Pharmaco 1998;151(2):236–44.
[17] Gao H, Chen C, Huang S, Li B. Quercetin attenuates the progression of monocrotaline-induced pulmonary hypertension in rats. J Biomed Res 2012;26(2):98–102.
[18] Chen H, Yang H, Xu C, Yue H, Xia P, Strappe PM, et al. Gene expression profiling of common signal transduction pathways affected by rBMSCs/F92A-Cav1 in the lungs of rat with pulmonary arterial hypertension. Biomed Pharmacother 2016;83:100–6.
[19] Lincoln TM, Wu X, Sellak H, Dey N, Choi CS. Regulation of vascular smooth muscle cell phenotype by cyclic GMP and cyclic GMP-dependent protein kinase. Front Biosci 2006;11:356–67.
[20] Vaillancourt M, Ruffenach G, Meloche J, Bonnet S. Adaptation and remodelling of the pulmonary circulation in pulmonary hypertension. Can J Cardiol 2015;31(4):407–15.
[21] Li Q, Youn JY, Cai H. Mechanisms and consequences of endothelial nitric oxide synthase dysfunction in hypertension. J Hypertens 2015;33(6):1128–36.
[22] Su JB. Vascular endothelial dysfunction and pharmacological treatment. World J Cardiol 2015;7(11):719–41.
[23] Frisco-Cabanos HL, Watanabe M, Okumura N, Kusamori K, Takemoto N, Takaya J, et al. Synthetic molecules that protect cells from anoikis and their use in cell transplantation. Angewandte Chemie 2014;53(42):11208–13.
[24] Mebarki M, Coquelin L, Layrolle P, Battaglia S, Tossou M, Hernigou P, et al. Enhanced human bone marrow mesenchymal stromal cell adhesion on scaffolds promotes cell survival and bone formation. Acta Biomater 2017;59:94–107.
[25] Dewachter C, Belhaj A, Rondelet B, Vercruyssen M, Schraufnagel DP, Remmelink M, et al. Myocardial inflammation in experimental acute right ventricular failure: Effects of prostacyclin therapy. J Heart Lung Transplant 2015;34(10):1334–45.
[26] Wynn TA, Chawla A, Pollard LW. Origins and Hallmarks of Macrophages: Development, Homeostasis, and Disease. Nature 2013;496(7446):445.
[27] Kumar S, Joos G, Boon L, Tournoy K, Provoost S, Maes T. Role of tumor necrosis factor-α and its receptors in diesel exhaust particle-induced pulmonary inflammation. Scientific Reports 2017;7(1):11508.
[28] Ha SJ, Lee CH, Lee SB, Kim CM, Jang KL, Shin HS, et al. A novel function of IL-12p40 as a chemotactic molecule for macrophages. J Immunol 1999;163(5):2902–8.
[29] Helmig S, Stephan P, Döhrel J, Schneider J. TNF-α mRNA Expression Correlates with TGF-β mRNA Expression In Vivo. Inflammation 2011;34(4):255–9.
[30] Yamasaki M, Kang HR, Homer RJ, Chapoval SP, Cho SJ, Lee BJ, et al. P21 regulates TGF-beta1-induced pulmonary responses via a TNF-alpha-signaling pathway. Am J Respir Cell Mol Biol 2008;38(3):346–53.
[31] Helbing T, Herold EM, Hornstein A, Wintrich S, Heinke J, Grundmann S, et al. Inhibition of BMP activity protects epithelial barrier function in lung injury. J Pathol 2013;231(1):105–16.
[32] Ito T, Okada T, Miyashita H, Nomoto T, Nonaka-Sarukawa M, Uchibori R, et al. Interleukin-10 expression mediated by an adeno-associated virus vector prevents monocrotaline-induced pulmonary arterial hypertension in rats. Circ Res 2007;101(7):734–41.
[33] Costa TA, Bazan SB, Feriotti C, Araújo EF, Bassi Ê, Loures FV, et al. In pulmonary paracoccidioidomycosis IL-10 deficiency leads to increased immunity and regressive infection without enhancing tissue pathology. PloS Negl Trop Dis 2013;7(10):e2512.
[34] Gomez D, Owens GK. Smooth muscle cell phenotypic switching in atherosclerosis. Cardiovasc Res 2012;95(2):156.
[35] Shanahan CM, Weissberg PL, Metcalfe JC. Isolation of gene markers of differentiated and proliferating vascular smooth muscle cells. Circ Res 1993;73(1):193–204.
[36] Clempus RE, Sorescu D, Dikalova AE, Pounkova L, Jo P, Sorescu GP, et al. Nox4 is required for maintenance of the differentiated vascular smooth muscle cell phenotype. Arterioscler Thromb Vasc Biol 2007;27(1):42–8.
[37] de Oliveira MG, Doro FG, Tfouni E, Krieger MH. Phenotypic switching prevention and proliferation/migration inhibition of vascular smooth muscle cells by the ruthenium nitrosyl complex trans-[Ru(NO)Cl(cyclam](PF6)2. J Pharm Pharmacol 2017;69(9):1155–65.
[38] Castle V, Varani J, Fligiel S, Prochownik EV, Dixit V. Antisense-mediated reduction in thrombospondin reverses the malignant phenotype of a human squamous carcinoma. J Clin Invest 1991;87(6):1883–8.
[39] Wang XQ, Frazier WA. The thrombospondin receptor CD47 (IAP) modulates and associates with α2β1 integrin in vascular smooth muscle cells. Mol Biol Cell 1998;9(4):865.
[40] Rashidi N, Tafazzoli-Shadpour M, Haghighipour N, Khani MM. Morphology and contractile gene expression of adipose-derived mesenchymal stem cells in response to short-term cyclic uniaxial strain and TGF-beta1. Biomed Tech (Berl) 2018;3:317–26.